Polyamides with a Choice of Structure and Crystal Surface Chemistry. Studies of Chain-Folded Lamellae of Nylons 8 10 and 10 12 and Comparison with the Other 2*N* 2(*N* + 1) Nylons 4 6 and 6 8

N. A. Jones, E. D. T. Atkins,* M. J. Hill, S. J. Cooper, and L. Franco

H. H. Wills Physics Laboratory, University of Bristol, Tyndall Avenue, Bristol BS8 1TL, U.K.

Received October 8, 1996; Revised Manuscript Received March 28, 1997[⊗]

ABSTRACT: Nylons 8 10 and 10 12 have been synthesized and crystallized as chain-folded lamellae from 1,4-butanediol and the results compared with previous studies on Nylons 4 6 and 6 8. In 2*N* 2(*N* + 1) Nylons, the lengths of the two alkane segments are equal and two different hydrogen-bonded sheet schemes are possible: progressive or alternating shear. At room temperature, Nylons 8 10 and 10 12 adopt the progressive scheme and the adjacent re-entry folds in the crystals must be in the alkane chain segments. In contrast, Nylons 4 6 and 6 8 lamellae, crystallized from the same solvent, exhibit the alternating hydrogen bonding scheme and each adjacent re-entry fold must contain an amide group. The transition in the chemical nature of the lamellar surface, from the amide fold to the alkane fold, occurs in passing from Nylon 6 8 to 8 10. Thus, the progressive hydrogen-bonded sheet/alkane fold structure is energetically more favorable, provided the alkane-folding geometry is sufficiently relaxed; this comes with increasing alkane segment length. For each hydrogen-bonded sheet structure there are still two principal intersheet stacking modes in lamellar crystals: the progressively sheared α-phase or the alternatingly sheared *β*-phase, both of which have been found in the 8 10 and 10 12 Nylons. The 2*N* 2(*N* + 1) Nylons have the choice of *four* possible structures. The melting points of solution grown crystals of Nylons 4 6, 6 8, 8 10, and 10 12 decrease with decreasing intrachain amide density. When lamellar crystals of these Nylons are heated, the two characteristic interchain diffraction signals move together and meet at their Brill temperature; for Nylon 10 12 it appears to be close to the melting point.

Introduction

The 2*N* 2(*N* + 1) family of Nylons, examples of which are shown in Figure 1, are special since each has an equal number of methylene units in both the diamine alkane and diacid alkane chain segments. Hydrogen bonding plays a key role in the crystallization and structure of aliphatic polyamides. Repetitive sequences of C═O···H−N hydrogen bonds occur between the chains, and these hydrogen bonds have the lowest energy when they are linear.[1−13]

Hydrogen-Bonded Sheets and Chain Folding. At room temperature, lamellar crystals of even−even Nylons are usually composed of chain-folded, hydrogen-bonded sheets.[1,2,4,7,11,12] The 2*N* 2(*N* + 1) Nylons are novel because there are two ways in which they can form sheets with linear hydrogen bonds,[1,2] as illustrated in Figure 2 for Nylon 8 10. In the first scheme (Figure 2a) the hydrogen bond positions, and therefore the chains, progressively shear by 13° parallel to the chain axis (*c*-direction). This hydrogen-bonding pattern is possible for all even−even Nylons and it is commonly found, for instance, in Nylon 6 6[3−5] and the Nylons of the *X* 4 family,[7] where it is the only possibility. If linear hydrogen-bonding is to be sustained in this arrangement, and the chains fold sharply (adjacent re-entry), then the folds have to be either in the diacid alkane or diamine alkane chain segments (see General Discussion). In the second scheme, the hydrogen bonds form an alternating pattern (Figure 2b) and for this structure to be sustained in adjacent re-entry chain-folded lamellar crystals, each fold must contain an amide group.[1] In chain-folded lamellar crystals of Nylons 4 6[1] and 6 8,[2] crystallized from 1,4-butanediol, it is this alternating hydrogen-bonded sheet/amide fold structure that is observed. Lamellar crystals of even Nylons, e.g., Nylon 4,[8] Nylon 6,[9] and Nylon 8,[10] also exhibit an alternating

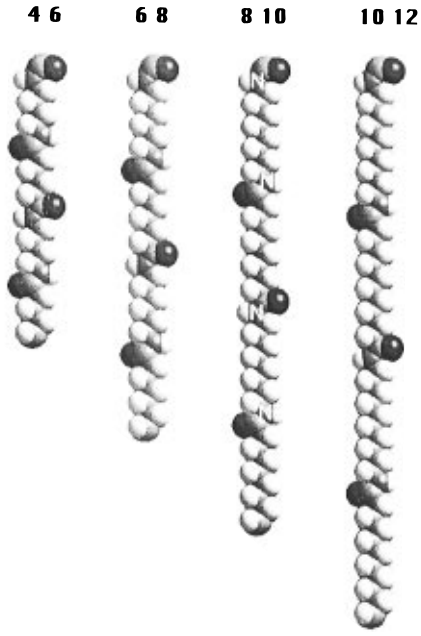

Figure 1. Computer-generated space-filling models of Nylons 4 6, 6 8, 8 10, and 10 12. The nitrogen atoms are labeled on Nylon 8 10 only. In each case there are equal numbers of methylene units in both the diamine alkane and diacid alkane segments. Note that the chains have no polarity in these synchephlic even−even Nylons; i.e., they are apolar. Color code: hydrogen, white; carbon, pale gray; nitrogen, medium gray; oxygen, dark gray.

* To whom correspondence should be addressed. Tel: (0)1179 288729 or 288733. Fax: (0) 1179 255624. E-mail: E.Atkins@bristol.ac.uk.

[⊗] Abstract published in *Advance ACS Abstracts,* May 15, 1997.

S0024-9297(96)01494-5 CCC: $14.00

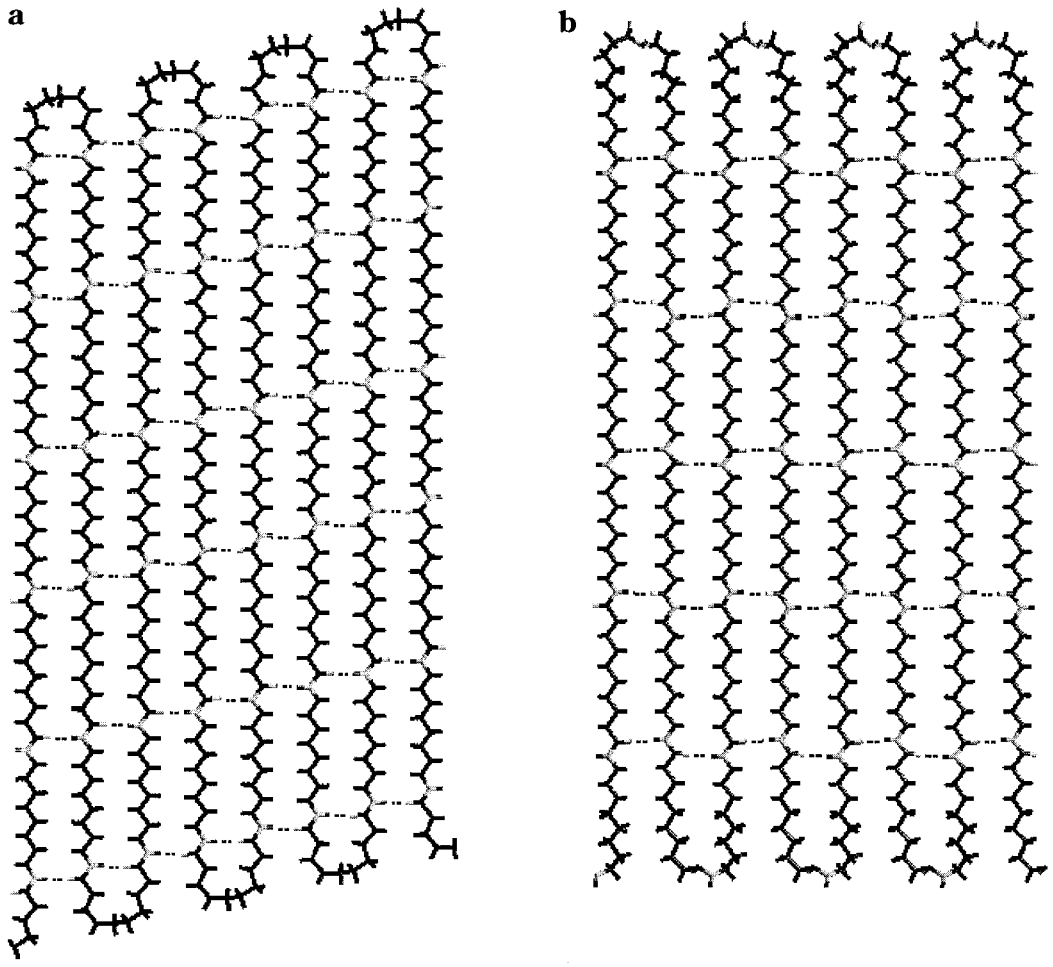

Figure 2. Different hydrogen-bonded schemes for chain-folded sheets of even−even Nylons using Nylon 8 10 as the example. (a) A view orthogonal to a single hydrogen-bonded sheet (*ac*-plane), illustrating the progressive shear of chains by 13°; similar to the structure of Nylon 6 6.[3] Whatever the sheet stacking arrangement (orthogonal to the sheet) the chain axis *c*-direction will always be inclined to the lamellar surface normal (α_p- and β_p-phases). The hydrogen bonds are indicated with dashed lines. (b) View orthogonal to a single hydrogen-bonded sheet (*ac*-plane), illustrating the alternating arrangement of hydrogen bonds, similar to the structure of Nylon 4 6.[1] The chains run orthogonal to the fold surface. They will remain orthogonal to the fold surface in β_a-phase lamellar crystals (Figure 3b) but will tilt in α_a-phase lamellar crystals (Figure 3a). Note, this alternating hydrogen-bonded sheet structure is different from the alternating hydrogen-bonded sheet structure described for the even Nylons.[8−10] The folding periodicity shown is commensurate with the interlamellar stacking periodicity as measured in the small-angle X-ray diffraction pattern of Nylon 8 10 (see Figure 6c and Table 1a). Color code: hydrogen and carbon, black; nitrogen and oxygen, gray.

hydrogen-bonded sheet pattern, but it should be noted that it is subtly different[2] from the alternating scheme described here (e.g., Figure 2b). For chain-folded lamellae of the even Nylons, their particular brand of alternating hydrogen-bonded sheet is the only arrangement possible.[8−10] In their case, the *same* hydrogen-bonded sheet pattern will be maintained whether the fold contains an amide group or folds via an alkane segment.

Stacking of Sheets. The chain-folded sheets are held together by van der Waals forces. Sheets where the chains shear progressively (Figure 2a) are often found to stack with a progressive shear, as illustrated in Figure 3a, and referred to as the α-phase by Bunn and Garner for the principal crystalline phase for Nylon 6 6.[3] The same sheets can stack with alternating shear, as shown in Figure 3b, and the arrangement is termed the β-phase.[3] Lamellar crystal preparations of Nylons 4 8, 4 10, 4 12, 6 10, 6 12, 6 18, and 8 12[11] and Nylon 12 10[12] can exhibit both of these phases. In both the α-phase and β-phase crystal forms, the chains shear progressively within the hydrogen-bonded sheets and both have triclinic crystallographic unit cells.[3,11,12]

Nylons 2*N* 2(*N* + 1) Have Four Choices. In the case of the alternating hydrogen-bonding scheme for 2*N* (2*N* + 1) Nylon sheets (Figure 2b), for which Nylon 4 6 is an example,[1] the two generalized sheet-stacking mechanisms are again possible, progressive or alternating, creating four possible generalized structures. In order to delineate between them we will use "p" and "a" to denote the progressive and alternating intrasheet hydrogen-bonding patterns, i.e. p-sheet and a-sheet, respectively, while α and β will refer to the progressive and alternating intersheet stacking, respectively[14] (see Figure 3). The two original Bunn and Garner[3] phases for Nylon 6 6 need to be defined more precisely as the α_p-phase and the β_p-phase. We have shown that the two different hydrogen-bonding schemes for the 2*N* 2(*N* + 1) Nylons give rise to two different sheet structures, and each of these must have a particular type of fold in order to maintain the hydrogen-bonded sheet pattern and adjacent re-entry chain folding. For these Nylons, this leads to an interesting result: the nature of the fold surface can be determined from the crystal structure (see General Discussion).

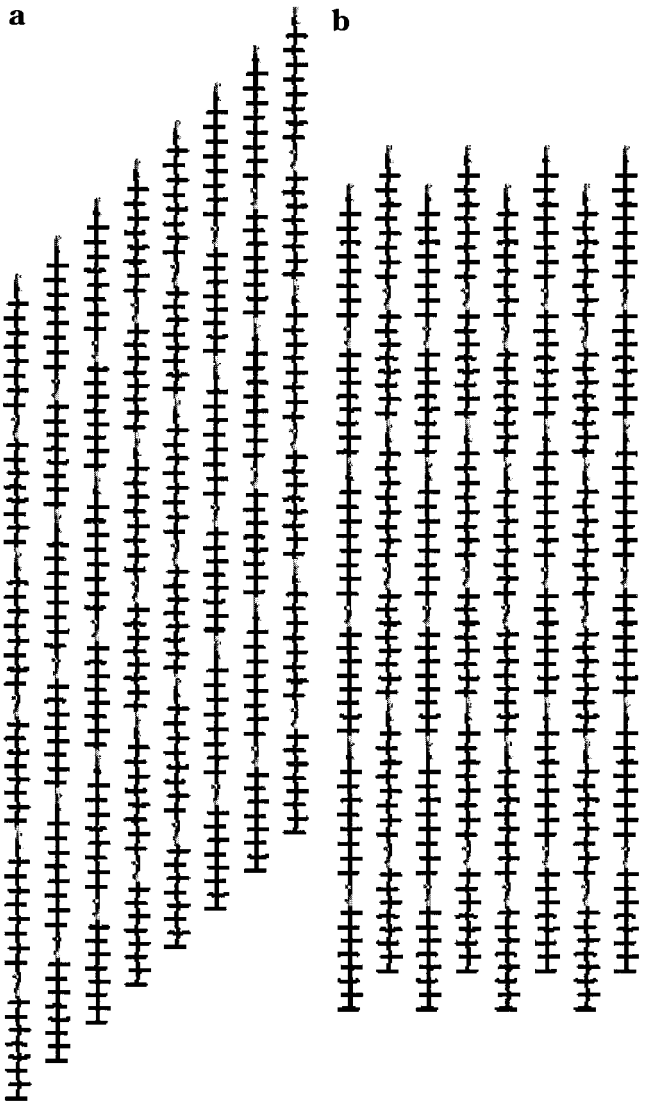

Figure 3. Stacking of the hydrogen-bonded sheets, using Nylon 8 10 as an example. Views in the *bc* plane showing (a) the progressive shear sheet stacking of α-phase crystals and (b) the alternating sheet stacking of the β-phase crystals. The chains will run parallel to the lamellar surface normal only if the sheets shown in Figure 2b are used (β_a-phase). Color code as in Figure 2.

In the case of the alternating hydrogen bond/amide fold structures of chain-folded lamellae of Nylons 4 6[1] and 6 8[2] the sheets stack with alternating shear to form monoclinic unit cells (since two of the angles are 90°); i.e., they are in the β_a-phase.

All the structures discussed above generate two strong and characteristic interchain diffraction signals, observed at 0.44 and 0.37 nm. These signals represent a projected interchain distance (actual value 0.48 nm) and the intersheet distance, respectively. It is known that as Nylon 6 6 crystals are heated, the two characteristic diffraction signals move together and meet at the Brill temperature.[13] The high-temperature phase of Nylon 6 6, above the Brill temperature, is pseudohexagonal,[2,6,13,15] as are the high-temperature phases of many other even−even Nylons,[2,6,7,11,12,16] including 4 6 and 6 8.[2] It has been shown that crystals of Nylons 6 6,[6] 6 8,[2] and 8[10] grow in the pseudohexagonal phase and revert to the higher density room temperature structure on cooling.

In this paper we report our observations of lamellar crystals of Nylons 8 10 and 10 12 and compare the results in detail with those previously obtained for Nylons 4 6[1,2] and 6 8.[2]

Experimental Section

Synthesis. Nylon 8 10 was synthesized by polymerization of an organic salt of 1,8-diaminooctane and 1,10-decanedioic acid. This is a standard method, described by Sorenson and Campbell.[17] To prepare the salt, approximately 52 mmol of 1,8-diaminooctane, dissolved in 12 mL of 100% ethanol, was slowly added dropwise to a solution of 50 mmol of 1,10-decanedioic acid in 60 mL of 100% ethanol. After addition was complete, the solution was left to cool for 24 h to ensure complete precipitation of the organic salt. The precipitated salt was isolated by filtration and repeatedly washed with 100% ethanol (to remove the excess diamine) before drying in a vacuum desiccator at room temperature. In order to prepare the polymer, 0.2 g of the organic salt was sealed into a glass tube under vacuum and partly polymerized at 195 °C for 24 h. The partially polymerized pellet was recovered and placed under vacuum within a heating block. The material was maintained at a pressure of 2−3 mbar at a temperature of 230 °C for 24 h.[17]

Nylon 10 12 was synthesized in a similar manner from a salt of 1,10-diaminodecane and 1,12-dodecanedioic acid. It was polymerized at 220 °C at 2−3 mbar air pressure for 24 h.

Characterization. The melting points, elemental analyses, and infrared spectra were consistent with expectations for the two Nylons synthesized. We did not prepare sufficient material to measure molecular weights directly with GPC. However, these Nylon samples exhibited high viscosity and oriented fibers could be drawn. Our previous experience leads us to believe that the molecular weights are in excess of 10 000.

Crystallization. Stock suspensions of chain-folded lamellar crystals were prepared by dissolving 20 mg of polymer in 100 mL of 1,4-butanediol at 190 °C; in each case the solution was allowed to cool to room temperature, during which time the polymer crystallized. Nylon 8 10 crystals were seeded[18] from a 0.002% w/v solution at 180 °C and crystallized at 110 °C for 48 h. Nylon 10 12 crystals were seeded from a 0.002% w/v solution at 190 °C and crystallized at 120 °C for 48 h. The crystal suspensions were hot-filtered at their crystallization temperatures. Sedimented mats of chain-folded lamellar crystals, suitable for X-ray diffraction experiments, were prepared by draining crystal suspensions through filter paper. The viscosity of the 1,4-butanediol was reduced by addition of methanol in order to increase the draining rate. The crystal mats were annealed in a vacuum oven at 100 °C for 24 h.

Transmission Electron Microscopy. Samples for transmission electron microscopy (TEM) were made by placing drops of crystal suspension on carbon-coated copper grids. The crystals were dried and annealed in a vacuum oven at 100 °C; the whole process took 24 h. Samples were examined in both imaging and diffraction modes, using a Philips EM400T TEM operating at 100 kV. Electron diffraction was performed with the electron beam parallel to the lamellar normal and with the sample stage tilted by 41° so that the electron beam was parallel to the chain axis.[5]

X-ray Diffraction. Both wide- and small-angle X-ray diffraction patterns were obtained using a point-collimated X-ray beam directed parallel to the surface of the crystal mat. X-ray diffraction photographs were obtained at room temperature using an evacuated X-ray camera and Ni-filtered Cu Kα radiation from a Philips PW2213 sealed beam X-ray generator operating at 35 kV and 40 mA. Calcite ($d_B = 0.3035$ nm) was dusted onto selected samples for calibration purposes. The measurements made as a function of temperature, were obtained using a monochromatized Cu Kα, point-collimated beam from an Elliot GX-21 rotating target X-ray generator and Siemens GADDS two-dimensional area detector. The samples were heated and the temperature controlled using a Linkham T300 hot stage.

Simulated X-ray diffraction patterns were computed from models using the Diffraction Module of Cerius 2, version 1.6

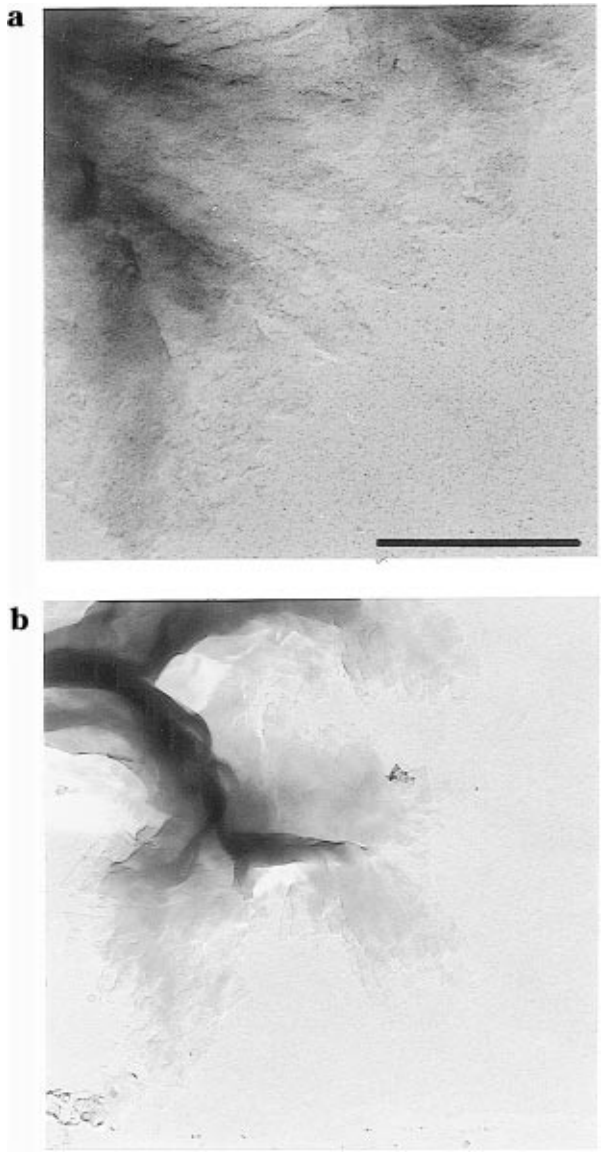

Figure 4. Transmission electron micrographs of lamellar crystals of Nylons 8 10 and 10 12, crystallized from solution in 1,4-butanediol, viewed orthogonal to their surfaces. Both pictures are at the same mangification; scale bar 1 μm. (a) Lamellar crystals of Nylon 8 10. (b) Lamellar crystals of Nylon 10 12. These crystals are in the form of large multilayers.

(Biosym/Molecular Simulations Inc.). The appropriate intensity correction factors were incorporated.

Differential Scanning Calorimetry (DSC). Melting temperatures of sedimented mats of Nylons 8 10 and 10 12 were measured using a Perkin-Elmer DSC7 flushed with nitrogen and with a heating rate of 10 °C/min.

Results and Discussion

Transmission Electron Microscopy. TEM imaging shows that the crystals of Nylons 8 10 and 10 12 are similar to crystals of many other Nylons[1,2,7−12] and grouped into sheaves (see Figure 4a,b).

Electron Diffraction. Parts a and b of Figure 5 show the electron diffraction patterns typical of the majority of our Nylon lamellar crystals (in these examples, Nylon 8 10) with the electron beam parallel to the lamellar normal and parallel to the chain axis (a tilt of 41°), respectively. Figure 5a is similar to that obtained from Nylon 6 6 α-phase crystals. There is a strong diffraction signal at 0.44 nm spacing (a projected interchain spacing) that indexes as the 100 on the Bunn

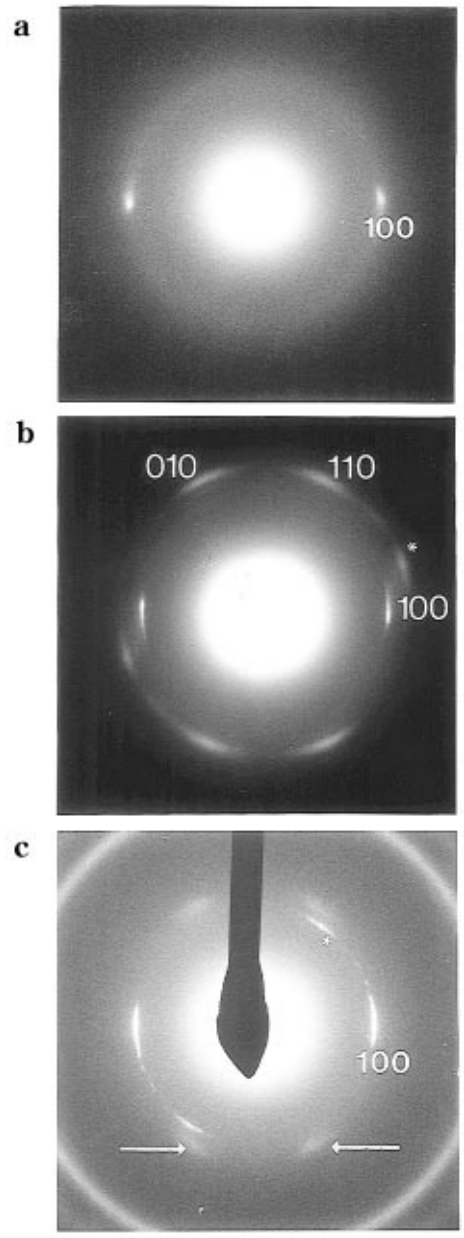

Figure 5. Examples of electron diffraction patterns obtained from Nylon lamellar crystals; similar results were obtained for both Nylon 8 10 and 10 12 crystals, apart from minor changes in the lattice parameters. (a) Obtained from a Nylon 8 10 chain-folded lamellar crystal preparation in the α-phase with the electron beam directed parallel to the lamellar normal. This phase gives rise to 100 signals only in electron diffraction. (b) The pattern obtained when the lamellae are tilted 41°, so that the electron beam is parallel to the chain axis. In this case *hk*0 diffraction signals are recorded. The signal marked * is from an overlaid crystal in a different azimuthal orientation. (Other diffraction signals associated with this overlaid crystal are not present since the tilt axis is not appropriate to bring them into the diffracting condition.) (c) Obtained from a Nylon 10 12 chain-folded lamellar crystal preparation in the β-phase with the electron beam directed parallel to the lamellar normal; the 020 and 120 (*b*-axis effectively doubled) diffraction signals (arrowed) appear in addition to the 100. The intensity of the 100 signal, relative to 020 and 120, is greater than expected for diffraction from the β-phase alone; thus, some α-phase is also present in this pattern. The outer diffraction ring is a Pt/Pd calibration ring. Note the relative diffuseness of the 020/120 diffraction signals. These signals represent the intersheet spacings that are controlled by weaker van der Waals forces. We have commented on this phenomena in Nylon structures previously.[2] The signal marked * is the 100 from an overlaid crystal in a different azimuthal orientation.

Table 1[a]

(a) X-ray Diffraction Data

Nylon 8 10						Nylon 10 12						
observed		α_p		α_a		observed		α_p		α_a		
electron diffraction	WAXD	index	calc	index	calc	electron diffraction	WAXD	index	calc	index	calc	error
0.443	0.444	100	0.443	200	0.443	0.443	0.445	100	0.443	200	0.445	0.003
0.372	0.370	010/110	0.370	010/210	0.372	0.372	0.371	010/110	0.371	010/210	0.371	0.003
	0.94	002	0.93	002	0.93		1.15	002	1.14	002	1.14	0.01
	1.86	001	1.85	forbidden			2.27	001	2.28	forbidden		0.04
	6.11	LX[b]		LX			7.65	LX		LX		0.05

(b) α_p and β_p Unit Cell Parameters for Nylons 8 10 and 10 12[c]

	α_p	β_p	α_a	β_a		α_p	β_p	α_a	β_a
	Nylon 8 10					Nylon 10 12			
a (±0.005 nm)	0.495	0.495	0.980	0.980	*a* (±0.005 nm)	0.495	0.495	0.980	0.980
b (±0.005 nm)	0.540	0.810	0.525	0.818	*b* (±0.005 nm)	0.530	0.810	0.515	0.820
c (±0.005 nm)	2.48	2.48	2.48	2.48	*c* (±0.005 nm)	29.8	2.98	2.98	2.98
α (±1°)	48.5	90	51.5	90	α (±1°)	50	90	52.5	90
β (±1°)	77	77	90	90	*β* (±1°)	77	77	90	90
γ (±1°)	64	67.5	70.5	65	*γ* (±1°)	64	67.5	70.5	65

[a] All dimensions are listed in nanometers. [b] LX = small-angle spacing. [c] Trial α_a and β_a unit cells used in simulations are also listed [d] The unit cell *a* and *β*-angle parameters were set at 0.495 nm and 77°, respectively, for α_p-phases, and at 0.980 nm and 90°, respectively, for α_a-phases, in accordance with the requirement that the hydrogen bonds should be linear within the sheets. For each Nylon, the *c*-value was set at $(0.125n - 0.02)$ nm, where *n* is the number of backbone bonds per chemical repeat, consistent with an all-trans conformation for the polyamide chains. (The 0.02 nm is subtracted because of the inclusion of the two nitrogen atoms in each backbone repeat.) The unit cell parameters *b*, α, and *γ* could then be calculated from the measured interplanar spacings. The resulting α_p unit cells are similar to that of the Nylon 6 6 α_p-phase (with the appropriate change in the *c*-value), differing by only ±0.02 nm in *b* and ±1° in the α and *γ* angles.

and Garner Nylon 6 6 α-phase crystallographic unit cell.[3,19] Figure 5c shows the electron diffraction pattern typical of a minority of our Nylon lamellar crystals (in this example, Nylon 10 12) with the electron beam parallel to the lamellar normal. In general features, it is similar to that obtained from Nylon 6 10 *β*-phase crystals.[11] This pattern shows a strong diffraction signal at 0.44 nm (again indexed as 100, but this time on the Bunn and Garner Nylon 6 10 *β*-phase crystal unit cell[3,19]) and diffraction signals at 0.37 nm, indexed as the combined 020 (intersheet) and 120 on the Bunn and Garner Nylon 6 10 *β*-phase crystal unit cell[3] (value of *b*-axis effectively doubled). The relative intensity of the 0.44 nm diffraction signal in Figure 5c is stronger than that expected for the *β*-phase alone, suggesting that the diffracting crystal contains some α-phase crystal as well as *β*-phase crystal.[11] The interatomic spacings and indexing of the observed electron diffraction signals are listed in Table 1a.

In some electron diffraction photographs, where the 0.37 nm diffraction signal is present, it is accompanied by second and third orders. This indicates that the polymer chains are, at most, only tilted slightly from the lamellar normal; this is consistent with the presence of *β*-phase crystalline lamellae. Nylons 8 10 and 10 12 chain-folded lamellar crystals, prepared as discussed above, produced both α-phase and mixed *β*-phase/α-phase crystals. However, in any given crystal preparation the α-phase was the predominant crystalline phase. Although *β*-phase crystals were always in the minority in both Nylon preparations, Nylon 10 12 crystal preparations showed the higher proportion of *β*-phase crystals. An example of the electron diffraction pattern from a tilted α-phase lamella, with the electron beam parallel to the chain axis, is shown in Figure 5b.[5] Both diffraction signals, at spacings 0.44 and 0.37 nm, respectively, are observed, as are the second and third orders. γ^* was measured directly from the diffraction pattern as $114 \pm 1°$ and was the same for both Nylons 8 10 and 10 12.

X-ray Diffraction. The wide-angle X-ray diffraction photographs from sedimented lamellar-crystal mats of Nylons 8 10 and 10 12, taken with the X-ray beam parallel to the mat surface, are shown in Figure 6a,b, respectively. The general features of the X-ray patterns are similar to those reported by Atkins *et al.*[4] for sedimented mats of Nylon 6 6, except, of course, that the *c*-spacings are greater, corresponding to the increased number of methylene groups. Although the X-ray patterns indicate α-phase crystal structures for both Nylons, with the chains tilted at a substantial angle to the lamellar normals, we cannot, on this evidence alone, decide if they are α_p-phase[3] or α_a-phase crystals. Also, in view of the electron diffraction results, we will need to allow for the possibility of some *β*-phase contamination of the X-ray diffraction data. On the basis of the measured interplanar spacings listed in Table 1a, unit cells were derived for both progressive and alternating intrasheet chain shear models (see Figure 2a,b). These unit cell parameters are given in Table 1b.

In Figure 6a,b the 00*l* diffraction signals occur on the meridian. In each Nylon, both the 001 and 002 signals are observed and the 002 has the stronger relative intensity. The ratio of the measured spacing of the 001 signal and the *c*-value, in each case, enables us to estimate the chain tilt from the lamellar normal. This is 41.4° ($\cos^{-1} = 1.86$ nm/2.48 nm) for Nylon 8 10 and 40.4° ($\cos^{-1} = 2.27$ nm/2.98 nm) for Nylon 10 12. These values are close to the value of 41.8° reported for Nylon 6 6 lamellar crystal mats[4] and fibers.[3] Using the unit cells derived for the α_p- and α_a-phases in Table 1b, we can compute the reciprocal angles between the prominent diffraction signals and the horizontal and vertical bisectors in the X-ray diffraction patterns. In order to simplify matters, we will discuss the results for Nylon 8 10 only; the conclusions for Nylon 10 12 are essentially the same. The relevant reciprocal angles for Nylon 8 10 are provided in Table 2. We know *a priori* that the *c**-axis is along the lamellar normal; vertical in Figure

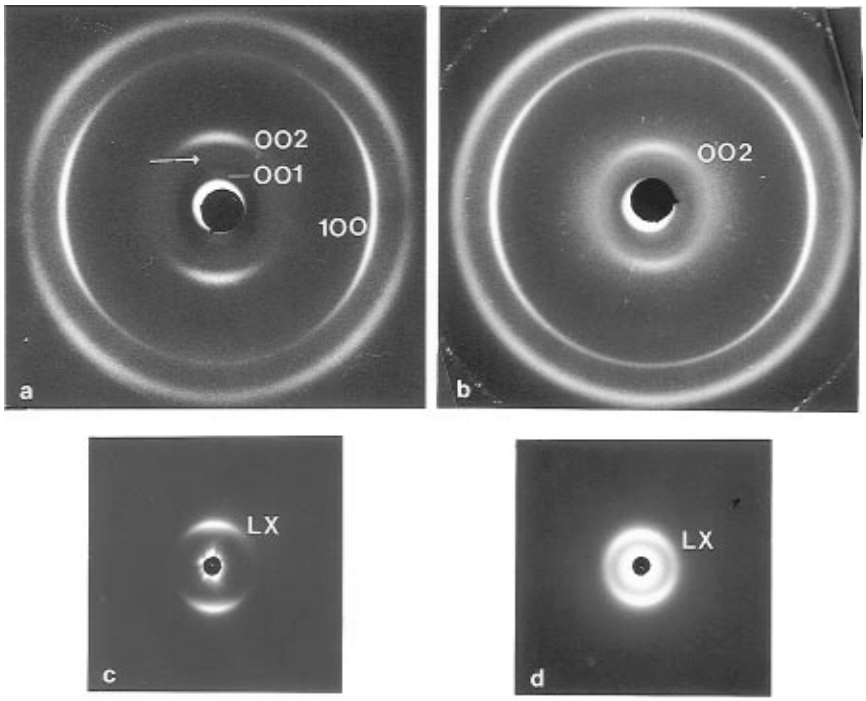

Figure 6. X-ray diffraction photographs of sedimented lamellar crystal mats, taken with the beam parallel to the mat surface and with the mat normal vertical. (a) Wide-angle X-ray diffraction from Nylon 8 10. The 00*l* diffraction signals are on the meridian; both 001 and 002 (labeled) are present, but the 002 has the greater relative intensity. A single subsidiary maximum (arrowed), commensurate with a (limited) lattice of three repeats is observed midway between the 001 and 002 meridional diffraction signals. The strong 100 arcs, split above and below the equator (horizontal bisector), overlap azimuthally so that we only see a single large arc centered on the equator. The combined 010/110 arcs generate the four-point pattern centered at about 40° above and below the equator. (b) Corresponding wide-angle X-ray diffraction photograph for Nylon 10 12. Note the position of the strong 002 meridional signal has moved toward the center of the pattern, compared with the Nylon 8 10 pattern (Figure 5a), by 18%, reflecting the increase in the *c*-dimension. The outer (spotted) ring is a calcite calibration ring. (c) Small-angle X-ray diffraction pattern from sedimented mats of Nylon 8 10. The meridional arc is at 6.11 nm and represents the interlamellar stacking periodicity. (d) Small-angle X-ray diffraction pattern from sedimented mats of Nylon 10 12; in this case the meridional arc occurs at a spacing of 7.65 nm.

Table 2. Reciprocal Space Angles for the Prominent X-ray Diffraction Signals for the Four Structures for Nylon 8 10

structure	α^* (deg)	β^* (deg)	γ^* (deg)	$[110]^* \wedge c^*$ (deg)
α_p (triclinic)	49.9	84.4	113.4	56.5
α_a (triclinic)	48.7	73.6	115.3	64.7
β_p (triclinic)	95.5	104.1	113.1	83.9
β_a (monoclinic)	90	90	115.0	90

6a. Thus for the α_p-phase, the diffraction signals should be angularly split (rounded to the nearest degree) either side of the equator as follows: the 100 by ±6° (90° − β^*), the 010 by ±40° (90° − α^*), and the 110 by ±33° (90° minus the angle between [110]* and *c**). The latter two signals occur at the same spacing, and therefore (within the inherent angular disorientation spread of the signals) they partially overlay and would be expected to center around 36°. Similarly, for the α_a-phase, the diffraction signals should be split either side of the equator by the following amounts: by ±16° for the 100, ±41° for the 010, and ±25° for the 110 (the partly overlaid last two centering around 33°). Visual estimations of the relative arc length of the 100 and the center of the overlaid 010/110 on the original X-ray diffraction photograph (Figure 6a) appear closer to the values expected for the α_p-phase; however, the results are not sufficiently accurate to entirely dismiss the α_a-phase.

A better clue to the detailed nature of the α-phase can be obtained from examination of the meridional diffraction series. Both 001 and 002 diffraction signals are observed, although the 002 is the more intense; also, a single subsidiary maximum is seen midway between the 001 and 002.[4] If the a-sheet structure shown in Figure 7b were present, we would not expect to see the 001 diffraction signal since the (001) planes would be perfectly halved by the sheet symmetry. This absence is inherent within the sheet structure (Figure 7b) which was constructed[20] using space group $P2_1/c11$, for which one extinction condition is: 00*l* for $l = 2n$ only. This condition is unaffected by the stacking arrangements of successive sheets in the full three-dimensional crystal structure.[20] In addition, with five (or more) identical planes containing carboxyl groups within, and parallel to, the lamellar surface (Figure 2b and small-angle interlamellar-stacking peak at 6.11 nm, Figure 6c), a single subsidiary maximum (commensurate with three repeats; see, for example, Atkins *et al.*[4]) is not expected. By analogy, the p-sheet shown in Figure 7a will generate a 001 diffraction signal, although much weaker than the 002 because intermediate "carboxyl-group-containing" planes occur close to the (001) plane halfway positions; also, since only three (001)-spaced planes occur (see small-angle X-ray diffraction discussion later), we would anticipate the observed single subsidiary maximum.[21] These arguments favor the α_p-phase for these crystal lamellae. Similar diffraction features and arguments apply to our results for Nylon 10 12.

In order to confirm our diffraction physics analyses and choice of the α_p-phase crystal structure, we have generated simulated X-ray diffraction patterns (SXDPs), using the commercially available Cerius 2 program for the straight-stem crystallography (thus the subsidiary maximum from the limited lattice will not appear), for both α_p- and α_a-phase crystals, based on the unit cell parameters listed in Table 1b. The SXDPs for Nylon 8

10 are shown in Figure 8a,b for the α_p-phase and α_a-phase crystals, respectively. The α_p-phase SXDP (Figure 8a) gives the better fit with the experimental X-ray diffraction pattern shown in Figure 6a; the 001 appears, the ratio of 001/002 intensity is well matched to that observed, and the positions and intensities of the other prominent (100, 010/110 pair) diffraction signals are correct. On the other hand, the α_a-phase SXDP (Figure 8b) does not generate the observed 001 diffraction signal and, furthermore, unwanted diffraction signals occur.

The small-angle X-ray diffraction patterns from sedimented mats of Nylons 8 10 and 10 12 are shown in Figure 6c,d, respectively. In both cases, a single meridional peak is observed, corresponding to the interlamellar stacking periodicity. The values (Table 1a) allow us to estimate the integer number of (projected) crystal structure repeats traversing each lamella; for both Nylon 8 10 and Nylon 10 12 this is 3 (Nylon 8 10, 6.11 nm/1.86 nm = 3.3; Nylon 10 12, 7.65 nm/2.27 nm = 3.4; which, in each case, has to reduce to 3 to allow for folds (see Figure 2a)).

Changes on Heating. Changes in the spacings of the characteristic 100 and 010 diffraction signals as a function of increasing temperature were monitored using X-ray diffraction for both α- and *β*-phase crystals. The spacings, as a function of temperature, are shown in Figure 9a,b for Nylons 8 10 and 10 12, respectively. Nylon 8 10 exhibits a Brill temperature below the melting temperature, as do Nylon 6 6,[6,13] the Nylon *X* 4 family,[7] and from the 2*N* 2(*N* + 1) group, Nylons 4 6 and 6 8[2] in particular. In Nylon 10 12, however, the two spacings approach convergence close to the melting temperature, as does Nylon 6 10 and a number of other even−even Nylons where the diacid alkane segment is longer than the diamine alkane segment.[11] The behavior of Nylons 4 6 and 6 8 on heating has previously been reported[2] but the data are reproduced in Figure 9c,d for comparison. The Brill temperatures and spacings for Nylons 4 6, 6 8, 8 10, and 10 12, together with the melting points for lamellar crystal mats, as measured by DSC, are listed in Table 3. The melting point (T_m) drops by about 100 deg between Nylon 4 6 (295 °C) and Nylon 10 12 (193 °C). In general terms, this would be consistent with with the decreasing amide density.[22,23] The Brill temperature (T_B) also drops, but the rate is only one half that of the fall in T_m, as the difference ($T_m - T_B$) reduces from 50 deg for Nylon 4 6 to what appears to be close to zero for Nylon 10 12 (see Table 3). Since it has been argued[15] that the Brill temperature is a consequence of a rearrangement of hydrogen bonds within the structure, T_B is more intimately related to the detailed interchain hydrogen bond arrangement rather than the average amide density, and there is no reason to expect T_B and T_m to mimic each other in detail. The Brill structure—the structure at and above the Brill temperature—occurs as the alkane segments become mobile (localized melting) and hydrogen bonds rearrange with a proportion flipping out of the fully hydrogen-bonded sheets to form intersheet hydrogen bonds,[10,11,15] whereas melting involves the breaking of the majority of the hydrogen bonds.

General Discussion

As mentioned in the Introduction, the 2*N* 2(*N* + 1) family of Nylons is unique within the even−even Nylon series, since the diamine alkane and diacid alkane segments are of equal length; this allows these polyamides to form two different types of chain-folded

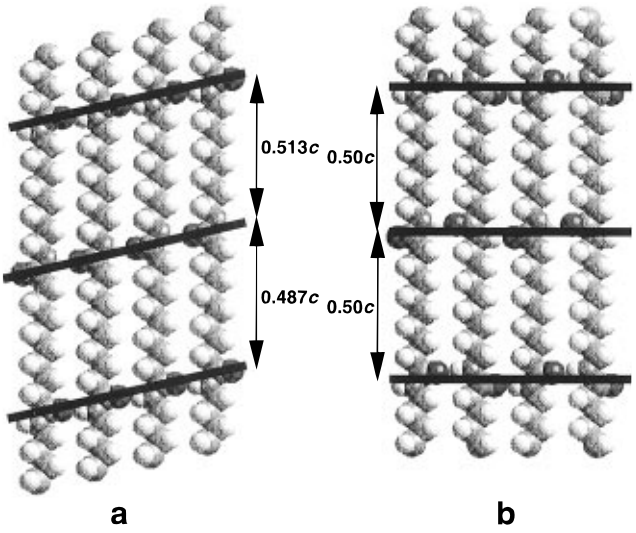

Figure 7. Space filling models of the straight-stem crystallography of Nylon 8 10 viewed orthogonal to the hydrogen-bonded sheets (*ac*-plane), showing planes of increased electron density (bold lines), i.e., those planes passing through the strongly diffracting carboxyl oxygen atoms. (a) In the p-sheet structure, the (001) diffracting planes are not exactly halved; they are split in the ratio 1.03/0.97, and consequently, the 001 diffraction signal is seen. (b) In the a-sheet structure the (001) planes are exactly halved, owing to the sheet symmetry, and therefore are systematically absent.

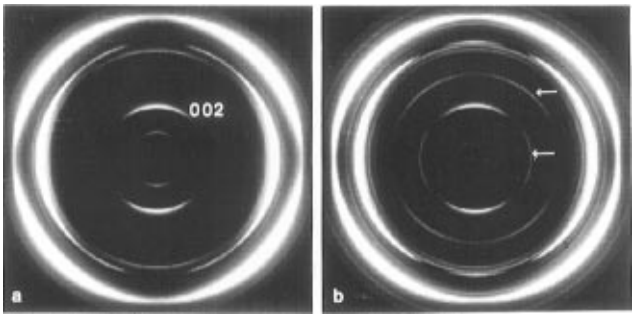

Figure 8. (a) Simulated X-ray diffraction pattern (SXPD) of the (straight-stem) crystal structure of α_p-phase crystals of Nylon 8 10 based on the unit cell parameters in Table 1a and with the *c**-axis vertical; thus, it can be compared directly with the X-ray diffraction photograph shown in Figure 6a. The 001 meridional signal occurs, and the ratio of the 001/002 intensities is correct. (b) SXDP of the (straight-stem) crystal structure of α_a-phase crystals of Nylon 8 10 based on the unit cell parameters in Table 1a and with the *c**-axis vertical. The 001 signal does not occur, and unwanted signals (arrowed) are generated.

hydrogen-bonded sheet structures: p-sheets or a-sheets (Figure 2a,b). Figure 10a shows that in order to preserve the intrasheet hydrogen-bonding arrangement within chain-folded p-sheets, diamine alkane segments align adjacent to neighboring diamine alkane segments, and with corresponding juxtapositioning for diacid alkane segments.[24] In this case, for the polymer chain to undertake intrasheet adjacent re-entry folding, the fold *must* occur via an alkane segment, either diamine alkane or diacid alkane,[4] and all the amide groups are embedded within the core of the hydrogen-bonded p-sheet. However in a-sheets, diamine alkane segments juxtapose diacid alkane segments, as illustrated in Figure 10b, and intrasheet adjacent re-entry folding can only happen if amide groups are sited at the apex of the folds,[24] thus removing them from the hydrogen-bonding scheme within the core of the a-sheet. Since each of the two chain-folded hydrogen-bonded sheets can

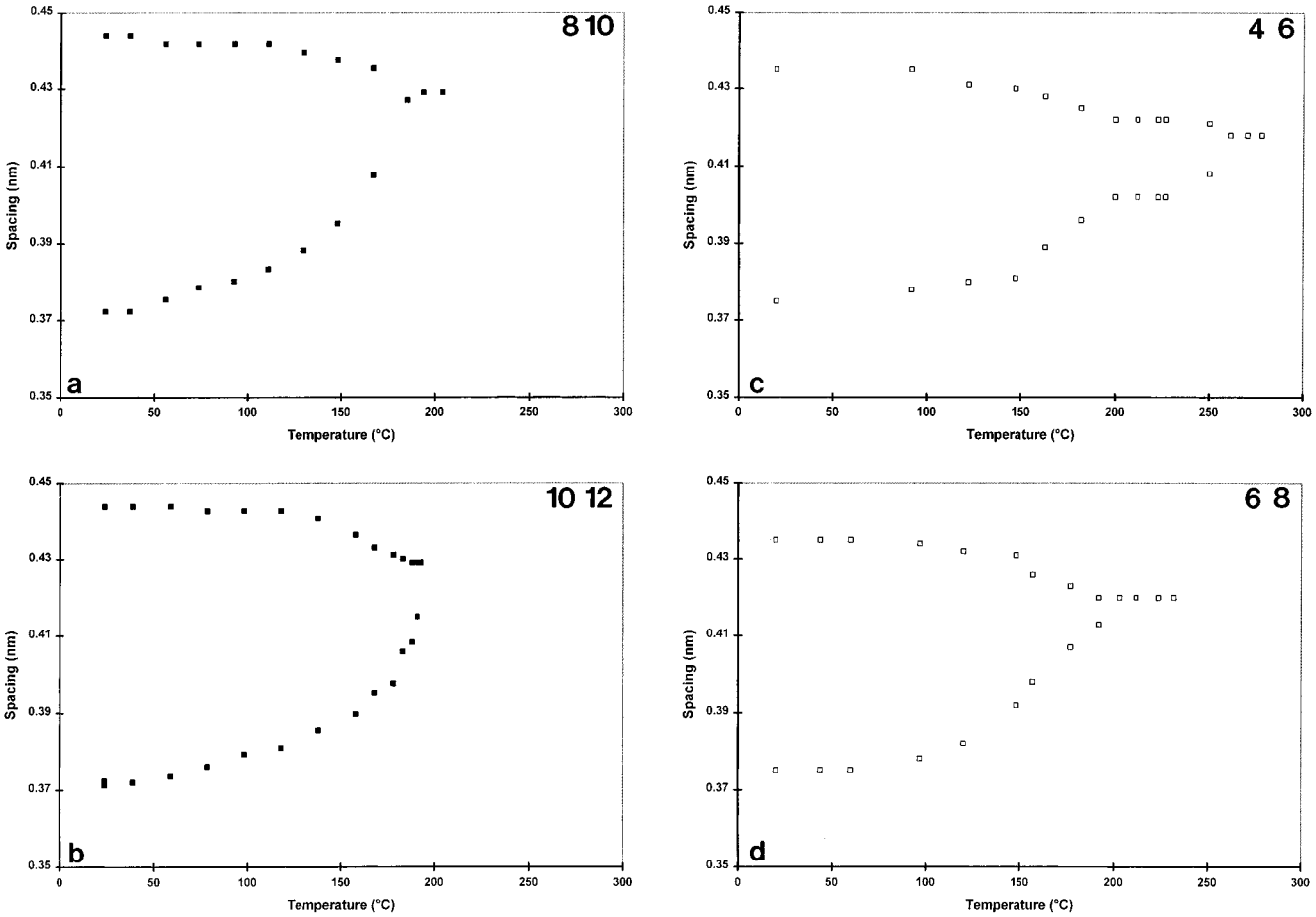

Figure 9. Graphs showing the changes in spacings of the two characteristic 100 and 010/110 diffraction signals, as the sedimented mats are heated from room temperature to the polymer melting temperature: (a) Nylon 8 10; (b) Nylon 10 12. These can be compared with the behavior of two other Nylon 2*N* (2*N* + 2) members: (c) Nylon 4 6 and (d) Nylon 6 8. It is known that these last two Nylons chain-fold with amide units in the folds. Key: (■) X-ray diffraction results; (□) electron diffraction results.

Table 3. Thermal Data and Brill Spacings

Nylon	mp (°C)	Brill temp (°C)	Brill spacing (nm)
4 6	295	245	0.420
6 8	234	203	0.420
8 10	210	185	0.420
10 12	193	*a*	*a*

[a] For Nylon 10 12, the two characteristic spacings converge close to the melting point, and there is uncertainty with respect to the Brill temperature (see curves in Figure 9b). It should be noted that Brill temperatures can vary a little with crystallization conditions.[6,10]

stack progressively or alternatingly, we have four possible types of crystal.

1. Alkane fold/p-sheets stacked with progressive shear: α_p-phase.
2. Alkane fold/p-sheets stacked with alternate shear: β_p-phase.
3. Amide fold/a-sheets stacked with progressive shear: α_a-phase.
4. Amide fold/a-sheets stacked with alternate shear: β_a-phase.

We have examined the published infrared spectroscopic literature for Nylons, for example.[25−28] In particular, the comprehensive and useful survey reported by Matsubara and Magill,[25] in which all classes of even−even, even, odd, odd−odd, odd−even, and even−odd have been studied. It is clear from this survey, that infrared spectroscopy is not able to satisfactorily delineate between the α_p- and α_a-type structures we have discussed for our Nylons; the similarity of the linear

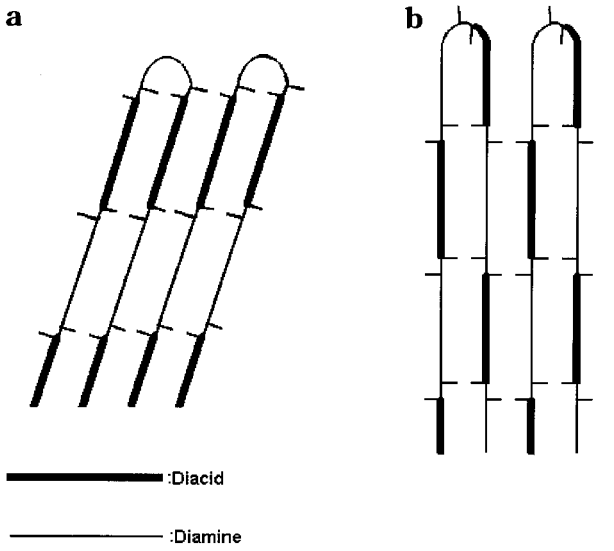

Figure 10. Schematic diagram to illustrate the juxtapositioning of diamine alkane and diacid alkane segments and the relationship to the chemical nature of the fold in (a) p-sheets and (b) a-sheets. The side arms indicate the position of the amide units.

hydrogen bonds shown in Figure 2a,b illustrates this point. Indeed, the reported infrared spectra for Nylon 6[25,27] and Nylon 6 6[25,28] have similar amide vibration bands.

Previous studies of lamellar crystals of Nylons 4 6[1] and 6 8[2] show that, when crystallized from 1,4-butane-

diol, these Nylons adopt the β_a-phase crystal structure. In contrast, lamellar crystals of Nylons 8 10 and 10 12 are predominantly in the α_p-phase, with a minority of β_p-phase, the latter usually in a β_p-phase/α_p-phase mixture. As already discussed, in chain-folded p-sheets the folds occur via alkane segments. We have shown elsewhere[8,7] that unstrained folds are not possible in alkane segments with less than four methylene units. For example, the p-sheet structure (if the sheet is to incorporate linear hydrogen bonds) is the only possibility for Nylon 4 4 and it has been found to crystallize in the α_p-phase.[7] The folds must contain alkane sequences, because there is no alternative folding scheme available to Nylon 4 4. Hence, the hydrogen bonds nearest the folds are strained, possibly broken,[7] because the diamine alkane sequences (four methylene units) are too short for unstrained folds; folding in the shorter diacid alkane segment (two methylene units) is completely ruled out. In the case of Nylon 4 6, both diamine alkane and diacid alkane segments consist of four methylene units. Folds in both alkane segments would be strained, as for Nylon 4 4. There is, however, another possibility open to Nylon 4 6 (although not to Nylon 4 4): chain-folded a-sheets can be achieved with unstrained folds. Certainly, alkane segment folds can form more easily as the lengths of the alkane segments increase; such folds would be strained for Nylon 4 6 lamellar crystals but not for Nylons 8 10 and 10 12. Nylon 6 8, with alkane segments of six methylene units, is probably marginal, as discussed below. (Alkane folds are completely ruled out for Nylon 2 4 where both diamine and diacid alkane segments are only two methylene units long.)

The question arises: does the fold determine the crystal structure, or does the crystal structure determine the fold? When the alkane sequences are sufficiently long for unstrained alkane folding (e.g., Nylons 8 10 and 10 12), the p-sheet structure is observed. However, when an alkane fold is strained (e.g., Nylon 4 6) the a-sheet structure is adopted. Thus, it appears that the p-sheet structure has a slightly lower energy than the a-sheet structure, and we might expect this for two reasons. Firstly, the interaction energy between amide groups will be at a minimum when the dipoles are aligned.[29] In the p-sheet structure the dipoles are aligned, but in the a-sheet structure they are inclined at a small angle to one another. Thus, the crystallographic straight-stem part of the p-sheet structure will have the lower energy. Secondly, if the fold contains an amide group, then this amide group will not be able to hydrogen bond within the straight-stem part of the crystal structure. This point is particularly pertinent for melt-crystallized chain-folded lamellae of the Nylon $2N$ $(2N + 1)$ family. In the case of Nylons crystallizing from solution, the solvent is able to hydrogen bond to amide groups in the fold and (partially) compensate for the loss of these hydrogen bonds in the whole chain-folded lamellar crystal. The overall energy difference between the two crystal structures (including folds) cannot be very great. Nylon 6 8, for which an alkane fold would be only slightly strained, has been observed to adopt both a- and p-sheet patterns (and therefore both amide and alkane folds, respectively) with differing crystallization conditions, for example, it was found in the β_a-phase when crystallized from 1,4-butanediol.[2] However, Slichter[30] studied fibers of Nylon 6 8 and found a mixture of structures. He concluded that both the α_p-phase and the β_a-phase were present. Dreyfuss[31] has published an X-ray diffraction pattern, obtained from a sedimented mat of Nylon 6 8, grown from a solution in a mixture of glycerine and water (Figure 1 in Dreyfuss[31]). This X-ray pattern suggests that the crystals are in an α-phase: unfortunately, the quality of the published photograph is not sufficiently good to allow a delineation to be made between α_p- or α_a-phase crystal structures. Thus, for Nylon 6 8, we see that the choice between the crystal structures is finely balanced. Experimental conditions, such as interaction with the solvent, will be likely to determine the resulting crystal structure.

The stacking of the chain-folded sheets varies within the $2N$ $2(N + 1)$ family. The a-sheets of Nylons 4 6 and 6 8 crystallize in the β_a-phase structure (see Figures 3b and 2b). The polymer chains are normal to the chain-folded surface, and the unit cells are monoclinic[1,2] with the two characteristic interchain (0.44 and 0.37 nm) diffraction signals. The p-sheets of Nylons 8 10 and 10 12 crystallize in both the α_p-phase (see Figures 2a and 3a), which is the predominant phase, and the β_p-phase (see Figures 2a and 3b), or mixtures of the two. These structures generate two different triclinic unit cells, but again, both with the two characteristic diffraction signals. Electron and X-ray diffraction data show that Nylon 10 12 lamellar crystals have a higher proportion of the minority β_p-phase compared with Nylon 8 10. To our knowledge, the α_a-phase has never been identified.

Knowledge of the internal structure (straight-stem crystallography) of lamellar crystals can reveal details of the chemical nature of the chain-folded surface, i.e., whether alkane or amide. As far as we are aware, there has been no direct determination of the surface chemistry of Nylon chain-folded lamellae. The fold-surface chemistry has, for some Nylons, been inferred from X-ray diffraction data,[4] neutron diffraction,[32] and computational modeling.[8] In $2N$ $2(N + 1)$ Nylons, the presence of a 001 diffraction signal, irrespective of the sheet stacking, confirms a p-sheet/alkane fold structure.

Conclusions

The $2N$ $2(N + 1)$ type Nylons, Nylons 8 10 and 10 12, have been synthesized and crystallized from 1,4-butanediol in the form of chain-folded lamellae. The structures and morphologies of these crystals have been studied and compared with Nylons 4 6 and 6 8. At room temperature, these lamellar crystals are composed of stacked chain-folded hydrogen-bonded sheets. We have shown that they can crystallize in two types of sheet: p-sheet (progressive) or a-sheet (alternating) and the sheets can stack with either a progressive shear to form α-phase crystals, or alternating shear to form β-phase crystals. Thus, four different crystal structures are possible which we describe as α_p, α_a, β_p, and β_a.

The results for Nylons 8 10 and 10 12 show that the crystals are predominantly in the α_p-phase, with a minority of β_p-phase, the latter usually mixed with α_p. In contrast, those $2N$ $2(N + 1)$ Nylons with alkane segments containing six or less methylene units, for example, Nylons 4 6[1] and 6 8,[2] were found to crystallize from 1,4-butanediol in the β_a-phase, i.e., in the a-sheet structure and with amide groups in the fold. Thus an interesting feature emerges from this family of four $2N$ $(2N + 1)$ Nylons, since these results show that as the length of alkane segments in the $2N$ $2(N + 1)$ Nylons increases, a change in the sheet structure occurs, with a consequent change in the chemical nature of the lamellar surface. We conclude that the p-sheet structure has a slightly lower energy than the a-sheet

structure. The p-sheet/alkane fold structure is preferred if both types of fold (alkane or amide) can be easily made. If, in a given 2*N* 2(*N* + 1) Nylon, the alkane segments are so short that strains would occur in the fold, then the a-sheet/amide fold structure is preferred. An interesting aspect, which we wish to highlight, is that the chemical nature of the folds is determined by the structure of the sheets: p-sheets have alkane folds and a-sheets have amide folds.

The melting temperatures of solution grown crystals drop by about 100 °C between Nylon 4 6 (295 °C) and Nylon 10 12 (193 °C) consistent with the decreasing linear density of hydrogen bonds. Although the Brill temperature also drops, the rate is approximately one-half. This difference in behavior reflects the different molecular processes controlling Brill temperatures and melting points.

Acknowledgment. We wish to thank the EPSRC for supporting this work, including a studentship (N.A.J.) and a postdoctoral fellowship (S.J.C.). L.F. acknowledges the support of the EU through a grant from the Human Capital Mobility program. We are grateful to Dr. Jarda Stejny for his help and advice regarding the synthesis of Nylons 8 10 and 10 12.

References and Notes

(1) Atkins, E. D. T.; Hill, M.; Hong, S. K.; Keller, A.; Organ, S. J. *Macromolecules* **1992**, *25*, 917.
(2) Hill, M. J.; Atkins, E. D. T. *Macromolecules* **1995**, *28*, 604.
(3) Bunn, C. W.; Garner, E. V. *Proc. R. Soc. London* **1947**, *189*, 39.
(4) Atkins, E. D. T.; Keller, A.; Sadler, D. M. *J. Polym. Sci.* **1972**, *A2*, 863.
(5) Holland, V. J. *Makromol. Chem.* **1964**, *71*, 204.
(6) Ramesh, C.; Keller, A.; Eltink, S. J. E. A. *Polymer* **1994**, *35*, 2483.
(7) Jones, N. A.; Atkins, E. D. T.; Hill, M. J.; Cooper, S. J.; Franco, L. *Macromolecules* **1996**, *29*, 6011.
(8) Bellinger, M. A.; Waddon, A. J.; Atkins, E. D. T.; MacKnight, W. J. *Macromolecules* **1994**, *27*, 2130.
(9) Holmes, D. R.; Bunn, C. W.; Smith, D. J. *J. Polym. Sci.* **1955**, *17*, 159.
(10) Atkins, E. D. T.; Hill, M. J.; Veluraja, K. *Polymer* **1995**, *36*, 35.
(11) Jones, N. A.; Atkins, E. D. T.; Hill, M. J.; Cooper, S. J.; Franco, L. *Polymer* **1997**, *38*, 2689.
(12) Franco, L.; Puiggali, J. *J. Polym. Sci., Part B* **1995**, *33*, 2065.
(13) Brill, R. *Z. Phys. Chem.* **1943**, *61*, 1353.
(14) When α or *β* are used in combination with p or a we will write p and a as subscripts, e.g., α_p.
(15) (a) Atkins, E. D. T. *Macromolecules '92: Functional Polymers and Biopolymers*, Canterbury, U.K., September 1992; Abstracts, p 10. (b) Atkins, E. D. T. *Macromol. Rep.* **1994**, *A31* (Suppls. 6 & 7), 691.
(16) Jones, N. A.; Cooper, S. J.; Atkins, E. D. T.; Hill, M. J.; Franco, L. *J. Polym. Sci., Polym. Phys.* **1997**, *35*, 675.
(17) Sorenson, W. R.; Campbell, T. W. *Preparative Methods of Polymer Chemistry*; Interscience: New York, 1961.
(18) Blundell, D. J.; Keller, A.; Kovacs, A. *Polym. Lett.* **1966**, *B4*, 481.
(19) The Bunn and Garner[3] triclinic unit cell parameters for Nylon 6 6 are $a = 0.49$ nm, $b = 0.54$ nm, c(fiber axis) = 1.72 nm, $\alpha = 48.5°$, $\beta = 77°$, and $\gamma = 63.5°$, and for Nylon 6 10 are $a = 0.495$ nm, $b = 0.54$ nm, c(fiber axis) = 2.24 nm, $\alpha = 49°$, $\beta = 76.5°$, and $\gamma = 63.5°$.
(20) The a-sheet was constructed using the space group $P2_1/c11$; thus, the second portion of each chain was formed using an inverse symmetry element, and the second chain (in the antiparallel pair) was generated by a screw axis parallel to the *a*-axis. The extinctions for this space group are $h00$ for $h = 2n$ and $0kl$ for $l = 2n$. This level of symmetry will be degraded in the α_a-structure since the a-sheets stack with progressive shear; however, the subset $00l = 2n$ extinction condition will still be preserved in the final structure.
(21) The occurrence of a recognizable subsidiary maxima fingerprint (in this case a single subsidiary maximum) demands that *all* the lamellae in the sedimented mat have the same well-defined thickness.
(22) Williams, R. S.; Daniels, T. *RAPRA Polyamide Rev.* **1990**, *3*, 33.
(23) Gedde, U. W. *Polymer Physics*; Chapman and Hall: London, 1995; p 173.
(24) In 2*N* 2(*N* + 1) Nylons, the folds in p-sheets must contain an odd number of alkane segments to meet the straight-stem registration criteria on adjacent re-entry. For the Nylons we have studied in this paper, one alkane segment is sufficient to make the fold. However, if the alkane segments are short, e.g. Nylon 2 4, then the folds might contain three alkane segments, similar to the *γ*-turns recently discovered in chain-folded lamellae of polypeptides (Panitch, A.; Matsuki, K.; Cantor, E. J.; Cooper, S. J.; Atkins, E. D. T.; Fournier, M. J.; Mason, T. L.; Tirrell, D. A. *Macromolecules* **1997**, *30*, 42. Krejchi, M. T.; Cooper, S. J.; Deguchi, Y.; Atkins, E. D. T.; Fournier, M. J.; Mason, T. L.; Tirrell, D. A. *Macromolecules*, in press). The folds in a-sheets must contain (sections of) both diamine alkane and diacid alkane segments. Since these alkane segments are of equal length, the amide group is positioned at the apex of the chain fold.
(25) Matsubara, I.; Magill, J. H. *Polymer* **1960**, *7*, 199.
(26) Elliott, A. *Infra-red Spectra and Structure of Organic Long-chain Polymers*; Richard Clay (The Chaucer Press) Ltd.: Suffolk, England, 1969.
(27) Arimoto, H. *J. Polym. Sci., Part A* **1964**, *2*, 2283.
(28) Garcia, D.; Starkweather, H. W. *J. Polym. Sci., Polym. Phys.* **1985**, *23*, 537.
(29) Duffin, W. J. *Electricity and Magnetism*, 4th ed.; McGraw-Hill: London, 1990; p 72.
(30) Slichter, W. P. *J. Polym. Sci., Polym. Phys.* **1958**, *35*, 77.
(31) Dreyfuss, P. *J. Polym. Sci., Polym. Phys.* **1973**, *11*, 201.
(32) Spells, S. J.; Sadler, D. M.; Keller, A. *Polymer* **1991**, *32*, 387.

MA961494G